Boron powder injection experiments in WEST with a fully actively cooled, ITER grade, tungsten divertor

K. Afonin, A. Gallo, R. Lunsford, S. Bose, Y. Marandet, P. Moreau, G. Bodner, H. Bufferand, G. Ciraolo, C. Desgranges, et al.

Nuclear Materials and Energy 40 (2024) 101724

Contents lists available at ScienceDirect

Nuclear Materials and Energy

journal homepage: www.elsevier.com/locate/nme

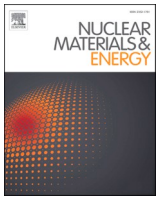

Boron powder injection experiments in WEST with a fully actively cooled, ITER grade, tungsten divertor

K. Afonin [a,*], A. Gallo [a], R. Lunsford [b], S. Bose [b], Y. Marandet [c], P. Moreau [a], G. Bodner [d], H. Bufferand [a], G. Ciraolo [a], C. Desgranges [a], P. Devynck [a], A. Diallo [b], J. Gaspar [e], C. Guillemaut [a], R. Guirlet [a], J.P. Gunn [a], N. Fedorczak [a], Y. Corre [a], F. Nespoli [b], N. Rivals [a], T. Loarer [a], P. Tamain [a], E.A. Unterberg [f], WEST team [1]

[a] CEA, IRFM, F-13108, Saint-Paul-Lez-Durance, France
[b] Princeton Plasma Physics Laboratory, Princeton, NJ, United States
[c] Aix-Marseille Université, CNRS, PIIM, UMR 7345, 13013, Marseille, France
[d] General Atomics, San Diego, CA, United States
[e] Aix Marseille Université, CNRS, IUSTI, Marseille, France
[f] Oak Ridge National Laboratory, TN 37830, United States

ARTICLE INFO

Keywords:
Plasma
Ipd
Soledge
Eirene
WEST

ABSTRACT

Reactor relevant fusion devices will use tungsten (W) for their plasma facing components (PFCs) due to its thermomechanical properties and low tritium retention. However, W introduces high-Z impurities into the plasma, degrading its performance. Different wall conditioning methods have been developed to address this issue, including coating of W PFCs with layers of low-Z material. Wall conditioning by boron (B) powder injection using an impurity powder dropper (IPD) is being studied in WEST. Two series of experiments were conducted since the installation of the new ITER grade full W divertor. During the first series in 2023 ~ 1 g of B powder was injected in total at a maximum rate of ~ 58 mg/s, both of which are three times greater than respective values in the initial WEST powder injection experiments. The second series of experiments included injection of B and BN powders for comparison of their effects on plasma performance. The presence of an instantaneous conditioning effect is suggested by visible spectroscopy measurements of low-Z impurity lines and a rollover of total radiated power past an injection rate of ~ 20 mg/s was observed. Presence of B coating layer formation is supported by the evolution of the average radiance of visible lines of B, W and oxygen (O). To understand B transport, an interpretative modeling workflow is employed, utilizing the SOLEDGE-EIRENE fluid boundary plasma code and the Dust Injection Simulator (DIS) code. Parameters like B perpendicular diffusivity and recycling coefficients are varied to match experimental results to see if the initial assumption of B sticking to the PFCs immediately after the contact with the wall is adequate for correctly modelling its distribution on the PFCs.

Introduction

Different wall conditioning methods in tokamaks with tungsten (W) first wall have been developed to prevent W contamination of the plasma, including coating of W PFCs with layers of low-Z material, such as in Glow Discharge Boronization (GDB). Wall conditioning with GDB is constrained by the necessity to turn off magnetic field coils to ensure uniform distribution of boron (B) coating, as well as the down time of 5–10 h for the duration of the procedure. Finally, GDB uses toxic diborane (B_2D_6) gas, which adds additional complexity and costs.

An alternative method of wall conditioning is the injection of low-Z powder, such as B and boron nitride (BN), during the pulse with an Impurity Powder Dropper (IPD) [1], providing wall conditioning in real time. B powder injection with an IPD as a conditioning method is being studied on multiple devices including DIII-D [2], EAST [3], AUG [14], KSTAR [15], LHD [16] and WEST [4,5], which is of particular interest

* Corresponding author.
E-mail address: kirill.afonin@cea.fr (K. Afonin).
[1] http://west.cea.fr/WESTteam.

https://doi.org/10.1016/j.nme.2024.101724
Received 22 May 2024; Received in revised form 29 July 2024; Accepted 14 August 2024
Available online 20 August 2024

Table 1
IPD drop rates in 2023 experiment.

Pulse #	Drop rates, mg/s	Duration of each injection, s
58047, 58048, 58,049	Reference pulses (no B powder)	0
58,050	0.0, 1.0, 3.4, 8.4	2.5
58,051	8.4, 12.4, 17.8, 24.7, 33.5, 44.5	2.5
58,053	17.8, 12.4	5
58054–58058	Disruption/cleaning pulse	0
58,059	17.8, 33.5, 58.0, 17.8	2.5

due to its long pulse capability and ITER grade lower divertor installed prior to the 2022–2023 campaign.

In WEST, pulses with B powder injection have been conducted previously, during the 2020–2021 experimental campaign, where ~ 310 mg of B powder were injected over 10 L-mode pulses [4]. Both transient and cumulative effects on the plasma parameters, such as main ion and impurity particle fluxes, line emission of light impurities and total radiated power have been reported, suggesting a cumulative conditioning effect and improved confinement during the injection [17].

For the experiments in 2023–2024 the following goals were set:

1. Evaluate the conditioning of the new fully actively cooled ITER grade tungsten divertor with powder injection;
2. Inject a similar amount of B to that typically used in GDB on WEST (~10 g);
3. Inject BN powder, which has not been done yet on WEST, to compare its performance to B powder considering the higher emissivity of N;
4. Find the smallest B/BN drop rate which positively and measurably affects the pulse, which can be relevant to avoid disruptions during continuous injection during long pulse discharges.

Experiment description

B powder experiments

The 2023 IPD experiments had approximately 1 g of B injected over 4 pulses. Three pulses without powder injection were used for reference. There were five additional pulses that didn't have powder injection due to early disruptions or their designation as an Ohmic cleaning pulse, which is necessary to restore machine conditions after a disruption. Injections were performed in lower single null (LSN) configuration, with 4.4 MW of lower hybrid heating power, with injections starting after 10 s of current plateau. Drop rates and injection durations are given in Table 1, and time traces of main plasma parameters are shown in Fig. 1.

The intrinsic impurity content appears to be lower in this experiment when compared to the previous WEST experiment, according to effective charge Z_{eff} measurements from the visible bremsstrahlung diagnostic (~2.5) in the reference pulses from 2022 and 2023 (Fig. 2). This

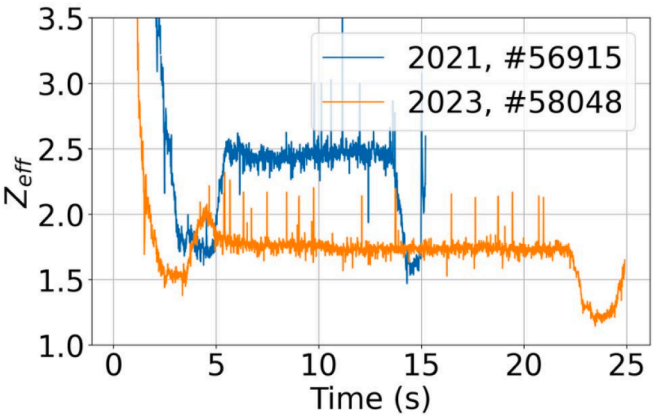

Fig. 2. Z_{eff} from line of sight in central plasma of visible bremsstrahlung diagnostic, pulses 56,915 & 58,048 (before powder injection).

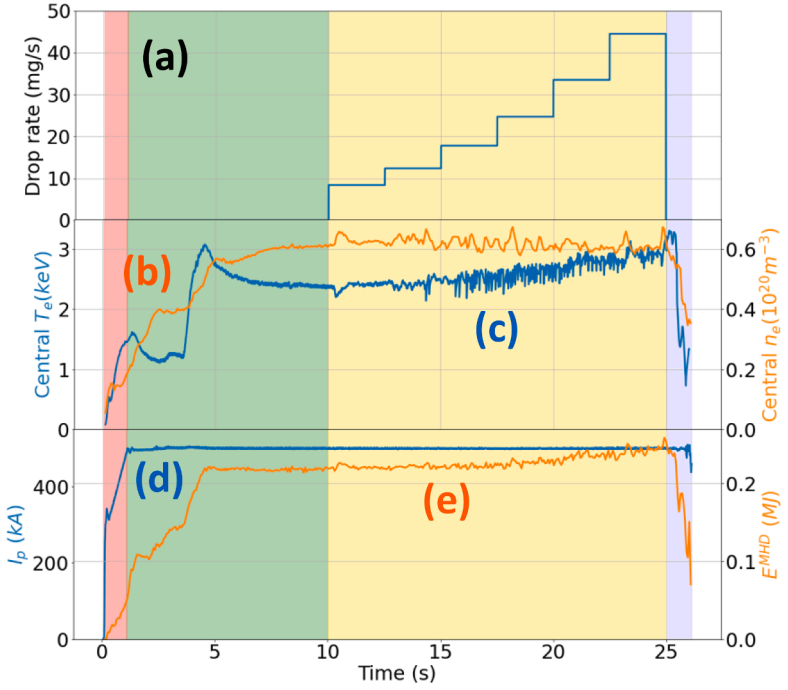

Fig. 1. Time traces of the programmed drop rate (a), central electron density and temperature (b,c), plasma current and total stored energy (d,e) in pulse #58051 in 2023 experiment. Color encodes pulse composition described in Table 1: current ramp-up in red, pre-drop phase in green, drop phase in yellow and ramp-down in purple. (For interpretation of the references to color in this figure legend, the reader is referred to the web version of this article.)

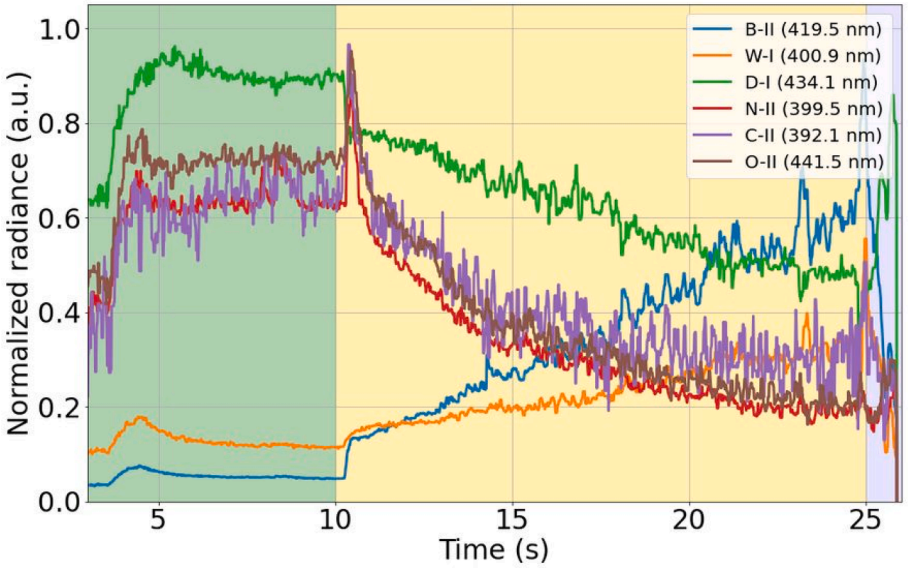

Fig. 3. Visible spectroscopy signals from the lower divertor in pulse #58051, normalized by line-integrated density at the lower divertor and scaled for readability (1.0 corresponds to time trace maximum in the presented time window). Background color is same as in Fig. 1.

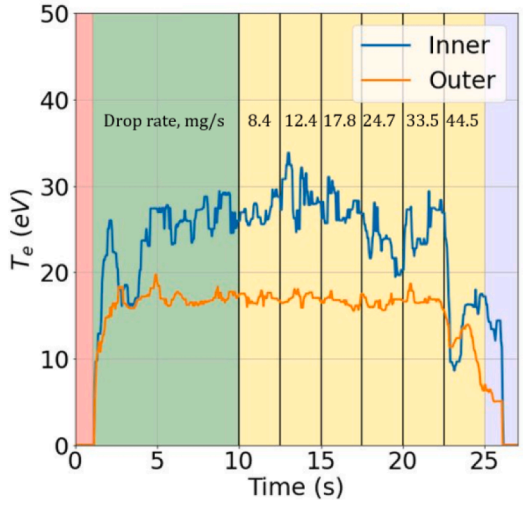

Fig. 4. Peak target electron temperature in pulse #58051 from 2023 measured by embedded Langmuir probes, background color is same as in Fig. 1.

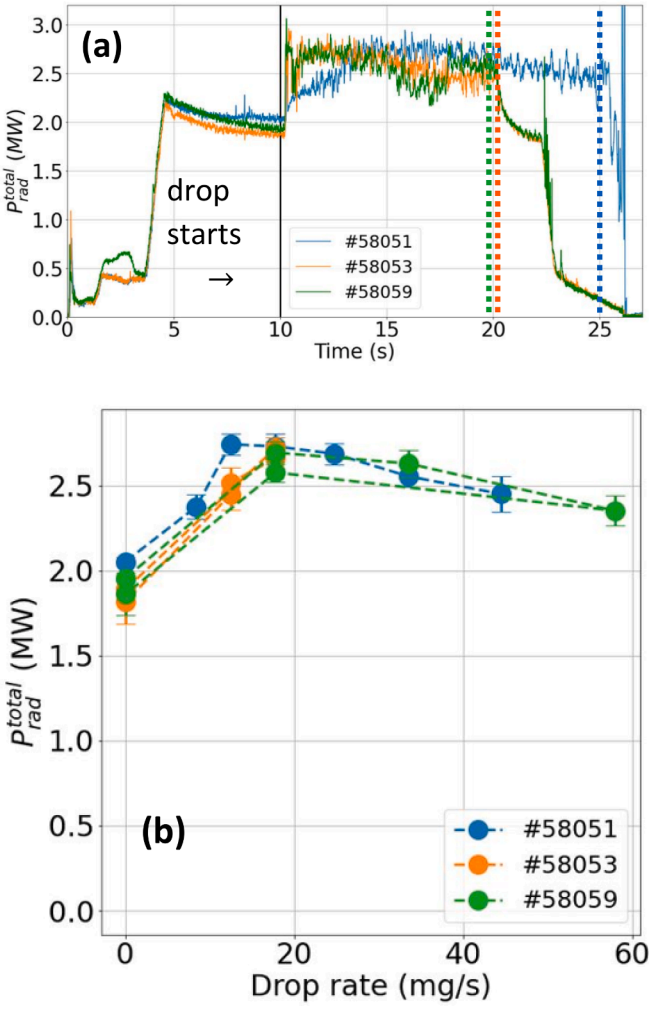

Fig. 5. Total radiated power from pulses with high drop rate as time traces (a) and as functions of drop rate (b). Dashed lines show the end of powder injection.

difference can be attributed to the new full-W divertor installed before the experiment in 2023, and it can explain the capability of the plasma to assimilate greater amount of B powder due to e.g. smaller sputtering rate of cleaner and smoother PFCs.

B powder injection experiments in 2024 had three pulse configurations: ohmic pulses, long pulses with 3 MW of LH heating, and pulses with 4 MW of input power similar to those from 2023. The injection rate of B and BN powder ranged from 0 to 4.8 mg/s.

Transient effects of B injection

Similar to the experiments in 2021, we observed real-time effects of B injection on wall conditioning via visible spectroscopy at the PFCs (lower and upper divertors, LFS inner bumper and HFS LH antenna). Time traces of spectral lines from an exemplary pulse at the lower divertor are shown in Fig. 3. The traces were normalized by line-integrated density at the lower divertor to account for the changes in electron density due to the changes in fueling and/or in ion recycling rates caused by B injection. The time trace of the B-II line indicates the increased amount of B at the lower divertor. D and light impurity signals

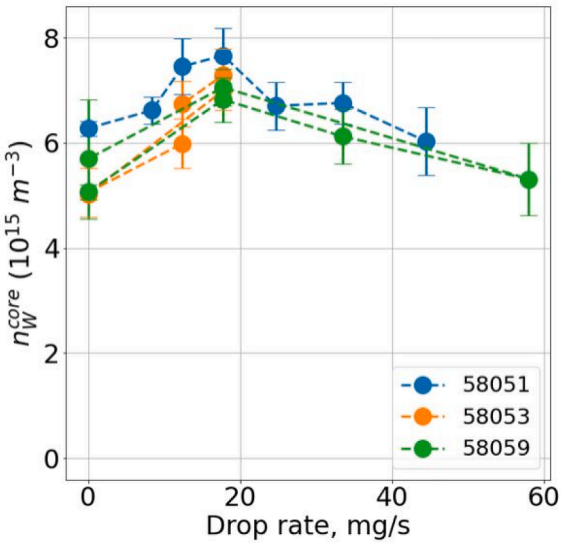

Fig. 6. Average tungsten density in core plasma as a function of drop rate in plasma pulses with high drop rate of B powder.

indicate lower recycling rates of the main ion and light impurity species. The W signal indicates increased sputtering of W by the injected B. The target electron temperature was mostly unaffected by the B powder injection, except for a sudden drop near the end of the injection at t = 22.5 s in #58051 (Fig. 4), suggesting a partial detachment of the inner leg. While GDB is usually performed as a method to bind O via the gettering effect [6], the spectroscopic data suggest that during the B powder injection carbon (C) and nitrogen (N) may also be trapped in the deposited B layers, which can be important considering that on WEST carbon (C) could still be an important contributor to W sputtering [7]. Similar to 2020–2021 experiments, improved confinement was also observed, e.g. increased stored energy E^{MHD} (Fig. 1e).

In addition, we observed a roll-over in total radiated power during B injection in 2023 past a drop rate $\mu \approx 20$mg/s, which was not previously observed in WEST IPD experiments (Fig. 5). The $P_{rad}^{total}(\mu)$ rollover follows the same distribution in both the first and the last pulses of the experiment (#58051 and #58059), indicating that the rollover is an effect of B injection on intrinsic impurity transport during the B drop and not a cumulative effect due to e.g. growth of B deposits.

Tungsten concentration n_W estimated from VUV spectroscopy and bolometry measurements [18] follows a very similar pattern (Fig. 6). The fact that n_W decreases past a certain B powder injection threshold similar to P_{rad}^{total} while W sputtering rate is consistently increasing with B drop rate indicates that W core density is lowered by affecting the transport in the boundary plasma via impurity injection. Speculatively, this effect may be attributed to the same mechanism as in N seeding experiments on WEST: stabilizing ion thermal gradient modes, leading to suppression of W transport into the confined plasma [8].

The behavior of the W visible spectroscopy line differs between the lines of sight at the inner and the outer targets. While the W-I radiance increases steadily at the outer target, it experiences a rollover at the inner target, albeit at a higher drop rate than in case of P_{rad}^{total} and core n_W density rollover (Fig. 7). This might be caused by the partial detachment of the inner leg of the plasma, also suggested by LP measurements of T_e (Fig. 3).

Cumulative effects of B injection

The cumulative conditioning effect of B powder injection was evaluated by averaging the visible spectroscopy signals in the pre-drop phase as the cumulative injected mass of B was increased. The change in radiance with cumulative mass of B (Fig. 8) suggests the formation of B layers on the inner bumper from pulse to pulse and degradation from disruptions (e.g. in #58054). When a disruption occurs, the B radiance is reduced and the W and O radiance is increased in the following pulse. This effect was observed on all PFCs, while being the most pronounced on midplane PFCs, observed by visible spectroscopy. Cumulative reduction of O-II line brightness can be speculatively ascribed to the fact that thicker B deposits increase the surface area of the PFCs, allowing for a more effective capturing of O via oxide formation.

Boron nitride (BN) injection effects

In 2024, for the first time BN powder was injected in WEST IPD experiments. Since the calibration of the BN feeder has not been yet performed, it is difficult to precisely estimate the injected quantities. In the absence of this, we assume that the drop rate mass-wise was similar for both B and BN, as the B signal during B powder injection was approximately twice that of the B signal during BN powder injection.

Assuming a similar drop rate, the transient effect of BN powder injection on O-II line radiance was found to be similar to the effect of B injection (Fig. 9b) for the given range of powder drop rates, even though the amount of B injected is noticeably different, as evidenced by Fig. 9a. This discrepancy between B injection rate and effect on O-II radiance in

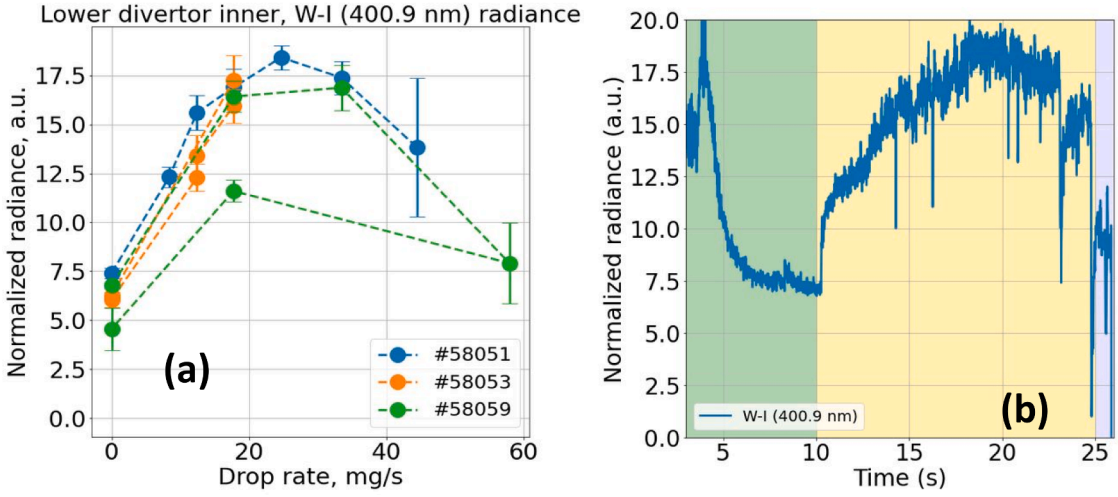

Fig. 7. Radiance of W-I line at the inner target of the lower divertor as (a) a function of the drop rate and (b) as a time trace in pulse #58051, normalized by lower divertor line-average electron density. Dashed lines in (a) show trajectory of the pulse in radiance/drop rate space.

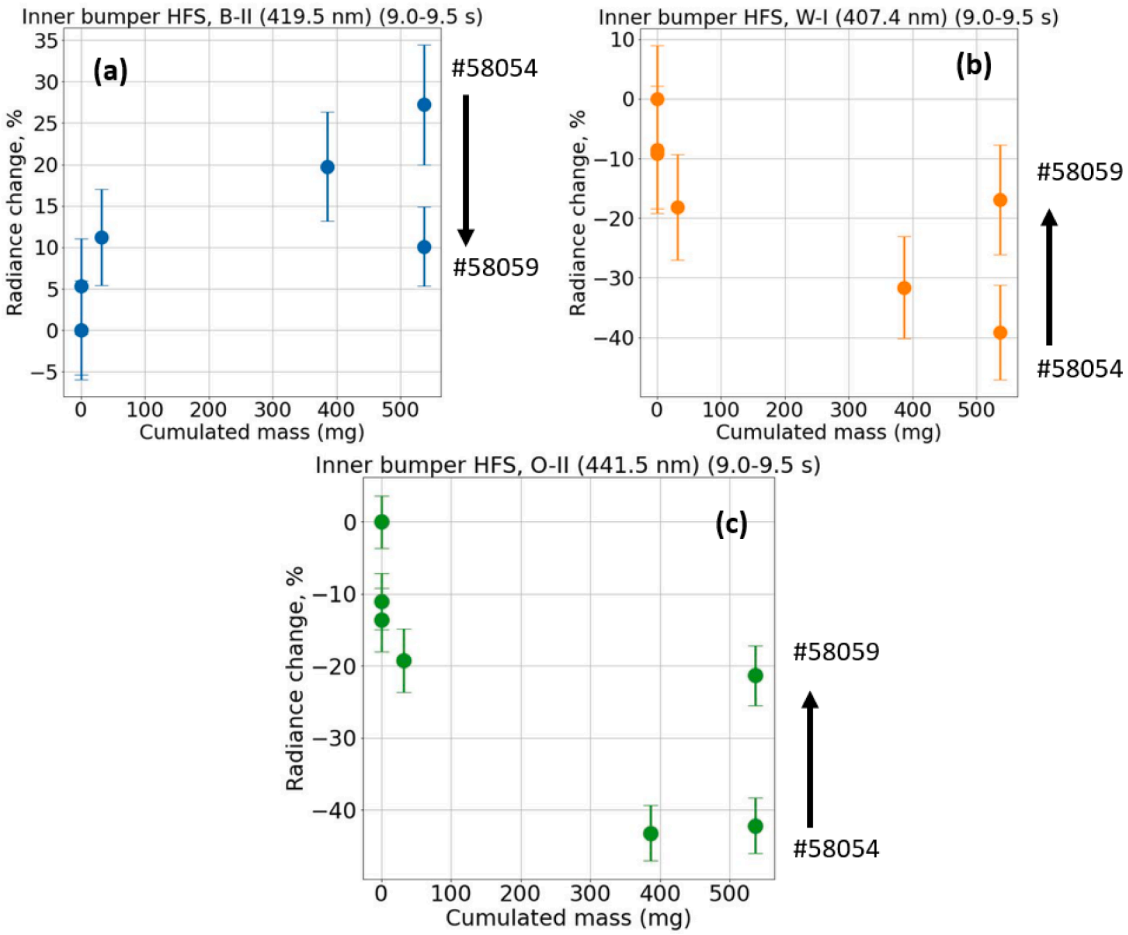

Fig. 8. Normalized radiance of B (a), W (b) and O (c) in pre-drop phase of pulses in 2023. Black arrows show dynamics of the measurements in response to a disruption that occurred in #58054.

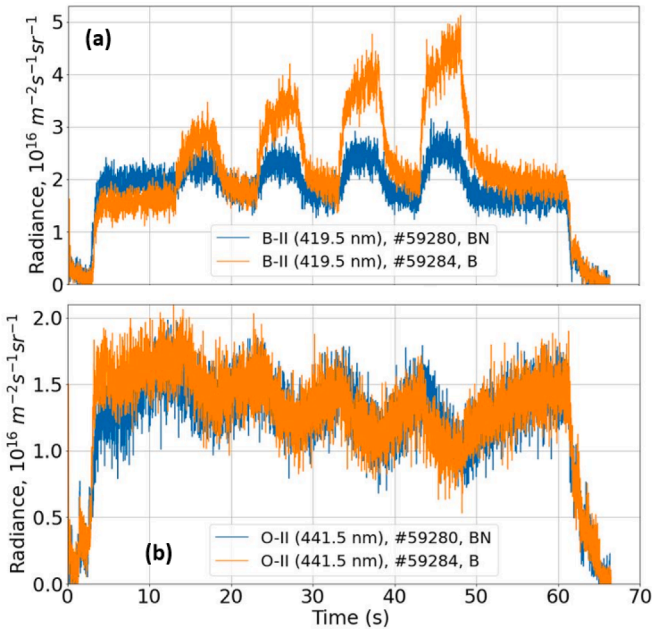

Fig. 9. B-II (a) and O-II (b) radiances in IPD experiments pulses with BN (a) and B injections.

B and BN injections remains unclear and should be investigated further at the higher drop rates.

Another motivation for using BN injection was to evaluate its impact on PFC heat loads compared to that of B powder (the strong emissivity of N has been shown to increase radiative losses [9]). Apparent temperature of inner target was measured with infrared cameras during the injection of both B and BN powders, but no significant difference was found between them in the investigated drop rate range (Fig. 10).

Interpretive modelling of B effect on the recycling of D and light impurities

In the experiments, the effect of B injection on the retention of D and low-Z impurities is not directly observable, and can only be inferred from the measurements of spectral line radiances and estimations of impurity fluxes with S/XB calculations. Interpretive modelling can help to fill the gaps in measurements by recreating similar plasma conditions in the numerical model provided with SOLEDGE/DIS workflow [5,10,11].

The numerical model was constrained by the: outer midplane electron density profile obtained from interferometry and the n_e, T_e at the divertor targets obtained from embedded Langmuir probes. Other plasma parameters were matched qualitatively: appropriate heating power was estimated using bolometry measurements and then varied to achieve quantitative match of the parameters above, as well as to match bolometry signal data from the experiments with the synthetic bolometry signals calculated with SYNDI synthetic diagnostic code [12], which, given P_{rad} 2D map and position of lines of sight of the bolometry

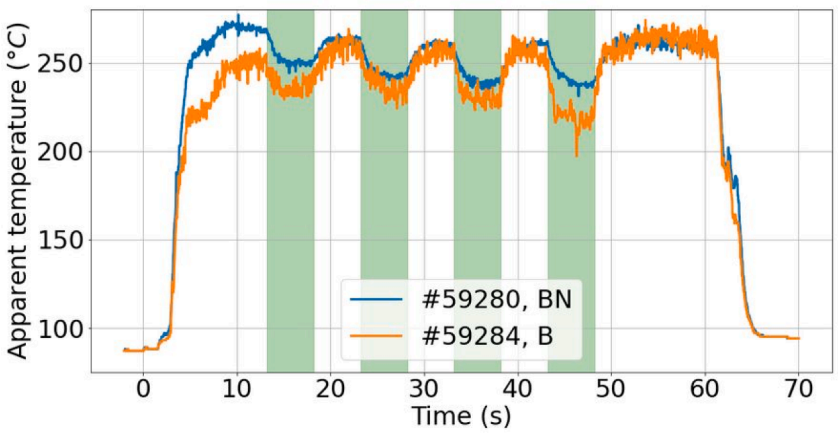

Fig. 10. Peak apparent temperature from a portion of inner target of the lower divertor in pulses with B and BN injection, 3 MW input power, with powder injection intervals in green. (For interpretation of the references to color in this figure legend, the reader is referred to the web version of this article.)

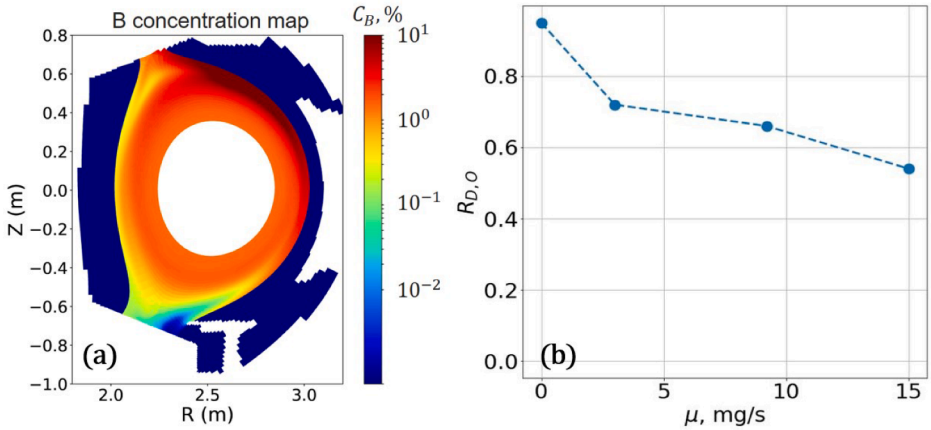

Fig. 11. (a) 2D distribution of the B concentration relative to D ion density in one of the simulations; (b)effect of drop rate μ on recycling coefficients of D, O in SOLEDGE-EIRENE/DIS modelling workflow.

detectors, computes synthetic bolometry signals. The effect of B injection on the O particle flux was estimated with the S/XB method in the experiments was additionally used to constrain the simulations (three-fold reduction of O flux at the lower divertor) by matching the bolometry measurements.

The resulting B ion distribution in one of the simulations is shown in Fig. 11(a). Recycling coefficient had to be varied depending on the boron source rate to match the experimental data. Interpretative modelling predicts a strong effect of B powder injection mass rate μ on the recycling coefficient $R_{D,O}$ (Fig. 11b), up to 15 mg/s. Simulations with powder injections above that limit had issues with particle balance convergence. The supposed decrease of $R_{D,O}$ in the experiments appears to be caused by the gettering of light impurities in B deposits, since similar experiments with N seeding [8,13] showed strong effects of impurity injection on divertor plasma configuration: increase of n_e and decrease of T_e at the targets, followed by a transition to X-point radiator regime. Similar effects of B injections on divertor plasma configuration took place in modelling if the reduction of recycling coefficients was not accounted for.

Conclusions

This paper summarizes the 2023 and 2024 IPD experiments on WEST and presents the effects of B powder injection on the plasma and PFCs. Cumulatively, B powder injection behaves similarly to GDB insofar that it facilitates capture of the light impurities, supposedly storing them in B deposits. In addition, B layers formed by powder injection seem to facilitate O capture after the injection, possibly due to higher surface area of the deposits relative to the bare W PFCs. During the drop, B powder injection increases W sputtering, but also appears to reduce the transport of W into the core, with the latter effect surpassing the former past a threshold of ~ 20 mg/s. The W transport effect is believed to be similar to the one occurring in N seeding experiments. In addition, B and BN powder injection reduces heat loads on the divertor targets and it may cause a partial detachment of the inner leg past a threshold of ~ 30 mg/s. Similar to previous studies, improves confinement is also observed during the B powder injection in the form of increasing central T_e.

An interpretive model was used in order to estimate the effect B powder injection has on the recycling of main ion and light impurities during the injection. Initial results describe major difference between the recycling coefficients in the pre-drop and drop phases, from 0.95 in pre-drop to 0.58 for the drop rate $\mu = 15$ mg/s. Future analysis should include particle flux comparisons between the computational model and the experimental estimates from S/XB analysis.

CRediT authorship contribution statement

K. Afonin: Writing – review & editing, Writing – original draft, Visualization, Validation, Software, Formal analysis, Data curation, Conceptualization. **A. Gallo:** Writing – review & editing, Supervision, Conceptualization. **R. Lunsford:** Software, Resources. **S. Bose:** Writing

– review & editing, Conceptualization. **Y. Marandet:** Writing – review & editing, Supervision, Conceptualization. **P. Moreau:** Supervision. **G. Bodner:** Writing – review & editing, Conceptualization. **H. Bufferand:** Software, Conceptualization. **G. Ciraolo:** Data curation. **C. Desgranges:** Data curation. **P. Devynck:** Data curation. **A. Diallo:** Writing – review & editing, Supervision, Conceptualization. **J. Gaspar:** Data curation. **C. Guillemaut:** Data curation. **R. Guirlet:** Data curation. **J.P. Gunn:** Data curation. **N. Fedorczak:** Data curation. **Y. Corre:** Data curation. **F. Nespoli:** Resources. **N. Rivals:** Software, Data curation. **T. Loarer:** Data curation. **P. Tamain:** Software. **E.A. Unterberg:** Data curation.

Declaration of competing interest

The authors declare the following financial interests/personal relationships which may be considered as potential competing interests: Kirill Afonin reports equipment, drugs, or supplies was provided by US Department of Energy. If there are other authors, they declare that they have no known competing financial interests or personal relationships that could have appeared to influence the work reported in this paper.

Data availability

Data will be made available on request.

Acknowledgments

This research was supported by the U.S. DOE under Contract No. DE-AC02-09CH11466 with Princeton University.

This work has been carried out within the framework of the EUROfusion Consortium, funded by the European Union via the Euratom Research and Training Programme (Grant Agreement No 101052200 – EUROfusion). Views and opinions expressed are however those of the author(s) only and do not necessarily reflect those of the European Union or the European Commission. Neither the European Union nor the European Commission can be held responsible for them.

References

[1] A. Nagy, et al., Rev. Sci. Instrum. 89 (2018) 10K121.
[2] A. Bortolon, et al., Nucl. Fusion 60 (2020) 126010.
[3] Maingi et al 2020 J. Fusion Energy.
[4] G. Bodner, et al., Nucl. Fusion 62 (2022) 086020.
[5] K. Afonin, et al., Nucl. Fusion 63 (2023) 126057.
[6] J. Winter, Plasma Phys. Control. Fusion 38 (1996) 1503.
[7] A. Grosjean et al 2023 Nuclear Materials and Energy 101385.
[8] X. Yang, et al., Nucl. Fusion 60 (2020) 086012.
[9] A. Bortolon et al 2019 Nuclear Materials and Energy 384-389.
[10] H. Bufferand, et al., Nucl. Fusion 55 (2015) 053025.
[11] F. Nespoli, et al., Phys. Plasmas 28 (2021) 073704.
[12] Devynck et al 2021 Physics Communications.
[13] P. Maget, et al., Plasma Phys. Control. Fusion 64 (2022) 045016.
[14] K. Krieger et al 2023 Nuclear Materials and Energy 101374.
[15] Gilson et al 2021 Nuclear Materials and Energy 101043.
[16] Nespoli et al 2022 Nature Physics, 18 350-356.
[17] G. Bodner, et al., Plasma Phys. Control. Fusion 66 (2024) 045022.
[18] R. Guirlet, et al., Plasma Phys. Control. Fusion 64 (2022) 105024.